Structural features and dynamic behaviour of the interlayer space of layered double hydroxide coatings

S. Soulé, Pierrick Durand, S. El-Kirat-Chatel, F. Quilès, C. Carteret

Materials Today Chemistry 35 (2024) 101897

Contents lists available at ScienceDirect

Materials Today Chemistry

journal homepage: www.journals.elsevier.com/materials-today-chemistry/

Structural features and dynamic behaviour of the interlayer space of layered double hydroxide coatings

S. Soulé [a,*], P. Durand [b], S. El-Kirat-Chatel [a], F. Quilès [a], C. Carteret [a]

[a] LCPME, UMR 7564, Université de Lorraine -CNRS, 405 Rue de Vandoeuvre, 54600, Villers-lès-Nancy, France
[b] CRM2, UMR 7036, Université de Lorraine−CNRS, BP 70239 Boulevard des Aiguillettes, F 54506, Vandœuvre-lès-Nancy, France

ARTICLE INFO

Keywords:
Layered double hydroxides
Coatings
Anion exchange
Dynamics
Stability

ABSTRACT

Layered double hydroxide (LDH) offer great potentialities to design functional coatings with customizable properties by exploiting their anion exchange properties. We investigated the anion exchange properties and expansion capacity of the interlayer space relating to the starting film morphology. ZnAl LDH coatings of different thicknesses and morphologies were first obtained by an *in situ* method using Al-based substrates. When the anion to intercalate is relatively bigger than the starting nitrates, the intercalation may be constrained by the initial LDH particle size and density composing the film. After optimising the morphology, the intercalation of three functional anions with potential antimicrobial properties was successfully achieved with an expansion of the interlayer space up to 150 % while holding the coating integrity. The release of the guest anion was studied by immersion in physiological saline solution. Finally, the possibility to regenerate the coating was demonstrated supporting the potential of these hybrid coatings for applications.

1. Introduction

Layered double hydroxides (LDH), also known as hydrotalcite-like compounds, consist of positively-charged brucite-like layers and charged-compensating anions. The general formula of LDH is given by $[M^{II}_{1-x} M^{III}_{x} (OH)_2]^{x+} [(A^{n-}_{x/n}). M\ H_2O]^{x-}$ where M^{II} (Mg^{2+}, Zn^{2+}, Fe^{2+}, Ni^{2+}, Co^{2+} ….) and M^{III} (Al^{3+}, Fe^{3+}, Cr^{3+} …) are metal cations, A^{n-} the interlayer anion and x defines the charge density of the layers. LDH are most commonly named as $M^{II}M^{III}$ LDH defining the nature of the two metal cations and sometimes additionally the nature of the anion (M^{II}-M^{III}-A). The possibility to vary the nature of metal cations, the M^{II}/M^{III} molar ratio, as well as the intercalated anions results in a large compositional flexibility for LDH with tuneable chemical and physical properties. This attractive feature has opened a large number of applications for LDH in different fields as catalysis [1,2], energy [3], water purification [4], and medicine [5].

For some applications in practical devices or functional coatings, LDH must be fabricated into supported films or self-supported membranes to maximize their functionalities while controlling the surface properties. This step can be very challenging as the synthesis methods developed for powder samples to control the material composition are not always transposable to the films.

There are two different approaches to elaborate LDH films. The former is a one-step method implying the LDH growth directly onto the support surface which can be achieved via several procedures. Inspired by the work of Clause et al. [6,7] on the LDH co-precipitate formation during γ-alumina impregnation with M^{2+} at neutral pH, Duan et al. [8] developed an *in situ* growth method for which the NiAl LDH grow directly from an aluminum-based substrate in presence of M^{2+} cations and ammonia as precipitant. The resulting films with thicknesses of several microns displayed crystallites with the *ab*-faces perpendicular to the substrate and very good adhesion to the substrate. The same method was used to elaborate MgAl [9] and ZnAl [10] LDH film on Al-based surface and have been extended to other metal-based surfaces yielding divalent ions upon oxidation such as zinc and copper [11], magnesium [12], and nickel [13]. As the metal support is the precursor of the M(II) or M(III) cations, the LDH film is dependent on the nature of the support restricting the achievable compositions. Urea was also used as precipitant to grow LDH film either on a metal substrate or other substrates [14–16] but only MgAl LDH films were obtained with this method. Moreover, as urea hydrolysis releases a mixture of ammonia and carbonate ions, the obtained films intercalated carbonate anions which cannot be easily replaced. Electrogeneration is an alternative way to grow LDH directly at an electrode surface through potentiostatic

* Corresponding author.
E-mail address: samantha.soule@univ-lorraine.fr (S. Soulé).

https://doi.org/10.1016/j.mtchem.2024.101897
Received 12 October 2023; Received in revised form 21 December 2023; Accepted 2 January 2024
Available online 13 January 2024

reduction of nitrate or sulphate ions, leading to hydroxide ions generation and LDH precipitation. Choosing an optimum deposition potential, salt concentrations and the pH of the plating solution are important parameters to control in order to obtain LDH as a pure phase in the film [17,18].

Another approach to elaborate LDH films is a two-step method requiring first the synthesis of LDH as nanoparticles or nanosheets in suspension and then the deposition using physical methods. Whereas there is no limitation in terms of LDH chemical composition or the nature of the substrate, the particles tend to orient parallel to the substrate and the adhesion is relatively low [19].

The perpendicular orientation offered by the LDH films elaborated by the *in situ* growth method can be advantageous for encapsulating and releasing active compounds. Moreover, such coatings can be prepared with nitrate anions intercalated in the interlayer galleries (LDH-NO_3). Nitrate anions are easily displaced due to the low interaction with the hydroxide layers [20] opening possibilities for film functionalisation.

LDH coatings have been widely reported for corrosion protection of metal surfaces such as Al, Mg, and their alloys. Besides their role as a physical protective film, the LDH coatings were used to trap aggressive chloride ions and release inhibitor ions based on the anion exchange capacity [21].

Tedim et al. [22] reported the beneficial corrosion protection of aluminum alloy 2024 (AA2024) with LDH-VO_x (prepared by anion exchange) compared to LDH-NO_3 and bare substrate under immersion in NaCl aqueous solution. Interestingly, the authors demonstrated that the active corrosion protection provided by vanadate ions did not clearly follow an expected 'concentration effect', with thin LDH films being more effective than thicker ones grown directly on the substrate. Unfortunately, the morphology of the film after intercalation of vanadates and after immersion was not characterised. They proposed the effect may be directly related to the stability of the underlying aluminum oxide film providing the high adhesion strength between the LDH film and the substrate.

The intercalation of low surface energy compounds like aliphatic carboxylates was also explored to obtain superhydrophobic surfaces and enhance the corrosion resistance. By intercalating sodium laurate into ZnAl–NO_3 LDH film grown on Al, the film morphology was greatly modified [23]. The film was demonstrated to be stable despite the presence of microscale hemispherical protrusions which were shown to not be attached to the substrate. Other studies [24,25] have reported morphological modifications due to the intercalation of laurate anions from a packed sheet to flowerlike structure, and platelets perpendicular to the surface were then disordered on the surface of Al substrate. Clearly, the intercalation of anions into LDH coating can significantly affect the film morphology and structure that must be controlled to have effective functional properties.

Despite these smart coatings have proven functionalities, the concept of LDH-container layers has not been widely extended to other field whereas they could have potential e.g. for biomedical applications. The main advantage of intercalating such compounds into LDH is a safer and more prolonged functionality. The intercalation of biologically active compounds into LDH films have been barely reported whereas many examples were found on LDH (nano)particles [26–30]. Liu et al. [31] have prepared an LDH coating intercalating an agent with anticancer and antibacterial abilities via a simple one-step hydrothermal method. The designed coating implant was effective at killing tumors and bacteria, inhibiting metastasis and resisting inflammation. The elaboration of a multifunctional LDH-based coating with anticorrosion and biocidal properties have also been investigated recently [32]. Even if the biocidal effect observed was consistent with the release of 2-mercaptobenzothiazole species as verified by a biological assay, the intercalation in the interlayer space had not been clearly demonstrated.

More generally, most of these studies dealing with the intercalation of anions into *in situ* grown LDH coatings demonstrated partial or total anion exchange but they almost did not address the influence of the film microstructure and morphology on the intercalating properties.

In this work, the exchange properties of ZnAl–NO_3 LDH films grown *in situ* onto Al-based substrates were investigated. The morphology of the LDH coating was controlled by varying the thickness of the Al-precursor layer. The intercalation of three organic anions (benzoate, cefotaxime and octanoate) was studied regarding their different size and potential functionalities. Antimicrobial, antiadhesive or antifouling properties could be obtained by developing the functionalisation of these surfaces which would be of great interest either as a release/uptake system or active coating for food packaging, self-disinfecting surfaces in medicine, waste-water treatment or marine environments.

The anion exchange properties were specifically investigated depending on the film thickness following the exchange dynamics, the structural and morphological modifications by Scanning Electron Microscopy (SEM), X-Ray Diffraction (XRD), Raman and Infrared (IR) spectroscopies. After optimising the starting film morphology, the expansion capacity of the interlayer space was studied at different scales (from the macroscopic to the atomic scale) with the intercalation of the organic anions. The stability of the functionalised coatings was addressed in physiological saline solution following the anion release kinetics. Finally, the reloading capacity of the film was evaluated as it could be a key parameter for practical applications. This experimental work should provide a fundamental understanding on the structural and dynamic behaviour of the interlayer space of layered double hydroxides coatings which would largely open the possibilities of applications.

2. Experimental section

2.1. Chemicals

Benzoic acid (97 %) and ammonium nitrate (98 %) were purchased from Acros Organics. Octanoic acid (>99 %) and zinc nitrate hexahydrate (98 %) were purchased from Sigma Aldrich, and cefotaxime sodium salt (98 %) from Alfa Aesar. 1 M sodium hydroxide solution was purchased from Carl Roth and NaCl (99.9 %) was purchased from VWR chemicals. Ammonia solution (1 wt%) was prepared from an ammonia solution (35 wt%) purchased from Fisher.

2.2. Synthesis of ZnAl–NO_3 LDH films

ZnAl–NO_3 LDH films were synthesized on aluminum coated silicon or glass substrates (13 mm diameter) using the *in situ* growth method adapted from Zhang et al. [10] with slight modifications. Silicon/glass substrates were washed with piranha solution and then coated with aluminum (both sides) using plasma sputtering (Q15OT S, Quorum). The thickness of the aluminium layer was varied: 30, 65 and 140 nm by modulating the deposition time.

An aqueous solution of 0.05 M of zinc nitrate and 0.6 M of ammonium nitrate was prepared and the pH was adjusted to 6.5 using 1 wt% ammonia solution. The solution was then transferred to a stainless-steel autoclave with a Teflon lining containing the aluminum-coated substrates hold vertically. The hydrothermal growth was carried out at 120 °C while adapting the time depending on the aluminum thickness (from 2 h to 5 h). The obtained LDH films were then washed with deionized water and ethanol and then dried using N_2 flow. The nitrate intercalated LDH film obtained from the Al-30, Al-65 and Al-140 substrate will be identified as ZnAl(30)-NO_3, ZnAl(65)-NO_3 and ZnAl(140)-NO_3.

2.3. Anion exchange with functional compounds

Nitrate anions occupying the interlayer space in the ZnAl LDH films were exchanged with three functional compounds (SI-Table 1). Benzoate, cefotaxime and octanoate anions were used in large excess to achieve the intercalation. For the intercalation of benzoate and octanoate anions, a solution (50 mL) of 1.6 mM of the corresponding organic acid

(benzoic or octanoic acid) was prepared adjusting the pH around 6 with 1 M sodium hydroxide. After 1 h of exchange under stirring and N_2 flow, the ZnAl-BZ or ZnAl–C8 film was rinsed with ethanol and dried using N_2 flow.

For the exchange with cefotaxime, ZnAl(65)-NO_3 LDH film was immersed into an aqueous solution (50 mL) of cefotaxime sodium salt (5.10^{-4} M, pH = 5) under stirring and N_2 flow. After 1 h, the film named ZnAl(65)-CFX, was rinsed with decarbonated water and dried using N_2 flow.

Each anion exchange experiment was repeated at least three times to ensure the reproducibility of the data.

2.4. Stability of the coating

The stability of the different hybrid coatings was studied by immersing vertically the samples into a 0.9 wt% NaCl aqueous solution (7 mL, pH around 6) under stirring. The release kinetics of benzoate and cefotaxime was monitored by UV–visible spectrophotometry measuring the absorbance in the 200–400 nm range. Aliquots (800 μL) of the solution were taken at regular times intervals over 3 h and then put back in the medium.

2.5. Reloading capacity

After 3 h immersion in 0.9 wt% NaCl solution, the benzoate anions in the ZnAl(65)-BZ coating were fully replaced by carbonates. The coating regeneration was attempted using the method proposed by Iyi et al. [33] using an acid-alcohol mixed solution to exchange the carbonates with nitrates.

The coating was immersed vertically in 50 mL of ethanol with 140 μL of a 0.15 M HNO_3 solution under stirring and N_2 flux for 45 min. The coating was then rinsed with ethanol and dried under N_2 flow.

2.6. Characterisation

Scanning electron microscopy (SEM) imaging. The morphology of LDH films was examined by using a JEOL JSM-IT500HR, with a field emission gun (FEG) and a voltage of 5–10 kV. Secondary electron detector (SED) was used for imaging. The elemental composition and Zn:Al molar ratio of LDH films was determined by Electron dispersive X-ray Spectroscopy using an Ultim Max 170 Oxford EDS detector coupled to the SEM. The accelerating voltage was set to 5 kV and the working distance to 10 mm.

X-ray Diffraction (XRD). The XRD measurements were performed using a Panalytical X'Pert Pro diffractometer equipped with a Cu tube, a Ge (111) incident-beam monochromator ($K\alpha_1$ = 1.5406 Å), and a X'Celerator detector mounted with the Bragg−Brentano geometry and automatic divergence slits. XRD patterns of the LDH films were measured in the ranges of 3–28° and 29–70°, with a step of 0,0167° for about 18 h. The size of the coherent domains in the directions perpendicular (L (003)) to the hydroxide layers of the obtained LDH were estimated from the full width at half maximum (FWHM) values of the respective diffraction reflections (003) using the Scherrer equation: $L = K.\lambda/\beta.\cos\theta$ where K is the Scherrer constant (0.9), λ is incident ray wavelength, β is the full width at half maximum in radians, and θ is the Bragg angle (rad).

Vibrational spectroscopies. The infrared analyses were performed on a Thermo Nicolet 8700 FT-IR and on a Bruker Vertex 70 v spectrometer, equipped with a KBr beam splitter and a DTGS detector. The infrared spectra of the LDH films were recorded under nitrogen flow in transmission mode. The spectral resolution was 4 cm^{-1} and the number of scans was 50 corresponding to a 1 min accumulation. Reference spectra of the anions in aqueous solution were recorded in the attenuated total reflection mode (ATR) between 4000 and 800 cm^{-1} using a nine-reflection diamond ATR accessory. The resolution of the single beam spectra was 4 cm^{-1} and the number of scans was 200, which corresponds to a 2 min accumulation.

Raman spectra were collected in the range of 50–4000 cm^{-1} with a Renishaw inVia Qontor spectrometer equipped with a Leica confocal microscope. Measurements were recorded using an Olympus × 50 objective. The instrument was equipped with an Edge filter to eliminate the Rayleigh scattering, 2400 grooves per millimetre grating, and the Renishaw Centrus detector. The excitation source was at 532 nm and the power was 3 mW at the sample. Spectra were baseline corrected with a polynomial function from Wire 5.4 software. The LDH film grown from Al-coated glass substrates were used for Raman characterisation to avoid the strong signal of Si in the Raman spectra. Each sample was analysed at several areas to check the uniformity of the coating.

X-ray Photoelectron spectroscopy (XPS). XPS measurements were recorded on a Kratos Axis Ultra X-Ray photoelectron spectrometer equipped with a microfocused (300 × 700 μm^2) monochromatic radiation (Al Kα source, 1486.6 eV) operating at 120 W under a residual pressure of about 10^{-9} mbar. The spectra were collected at a take-off angle of 90° with a pass energy of 20 eV. Charge compensation was applied by flooding low-energy electrons. All spectra were energy-calibrated assigning the adventitious carbon C 1s a binding energy of 285.0 eV. Spectra were mathematically fitted with Casa XPS software using a least-squares algorithm and a nonlinear Shirley-type background. The fitting peaks of the experimental curves were defined by a combination of Gaussian (70 %) and Lorentzian (30 %) distributions.

Chemical analysis. To quantitatively evaluate the amount of LDH grown on the substrates, the amount of zinc and aluminum were measured by Inductively Coupled Plasma Mass Spectroscopy (ICP-MS, Agilent-7800). After the film dissolution into 25 mL of 1 wt% HNO_3 under sonication, each solution was diluted 50 times before analysis. The calibration curve in the range 20–400 ppb has been established using zinc (Sigma-Aldrich) and aluminium (SCP Science) standards for ICP. The detected isotopes were ^{66}Zn and ^{27}Al.

UV–visible spectrophotometry. The concentration of organic anions released when studying the coating stability was quantified when possible by UV–visible spectrophotometry. The absorbance of the medium was measured with a Cary6000i spectrometer in the UV range 200–400 nm with a spectral bandwidth of 2 nm using quartz cells (5 mm). The concentration was evaluated considering the absorbance measured at 224 nm for benzoate and 234 nm for cefotaxime solutions.

3. Results and discussion

3.1. Control of the coating morphology

Nitrate intercalated ZnAl LDH films (ZnAl–NO_3 LDH) were prepared by adapting an *in situ* growth method described elsewhere [10]. While the film morphology and thickness can be controlled by varying the concentration of Zn salt and the hydrothermal conditions [34] (temperature and time) using Al-based substrates, another possible approach is to tune the thickness of the aluminum layer, which is the Al precursor for the LDH co-precipitation.

SEM images of ZnAl–NO_3 LDH films, named ZnAl(30)-NO_3, ZnAl (65)-NO_3, ZnAl(140)-NO_3, obtained from the different Al-coated Si substrates (30 nm, 65 nm and 140 nm, respectively) are shown in Fig. 1. The films showed the typical morphology observed when using the *in situ* growth method with slightly curved platelets mainly oriented perpendicular to the substrate [8]. By increasing the Al layer thickness, the film became denser with more and larger particles. This evolution had already been observed by Cao et al. [34] when modulating the hydrothermal time during the growth of ZnAl LDH on aluminum plates. In fact, the thicker the Al layer is, the higher the amount of Al^{3+} ions released in solution is. Higher Al(III) concentration lead to a significant increase of the film thickness (related to the particles size) from 1.5 μm to 1.9 μm and 2.4 μm starting with 30 nm, 65 nm and 140 nm thick Al layer (Fig. 1 d-f), respectively, whereas the platelets thickness slightly changed. The growth rate higher in the *ab*-direction compared to the

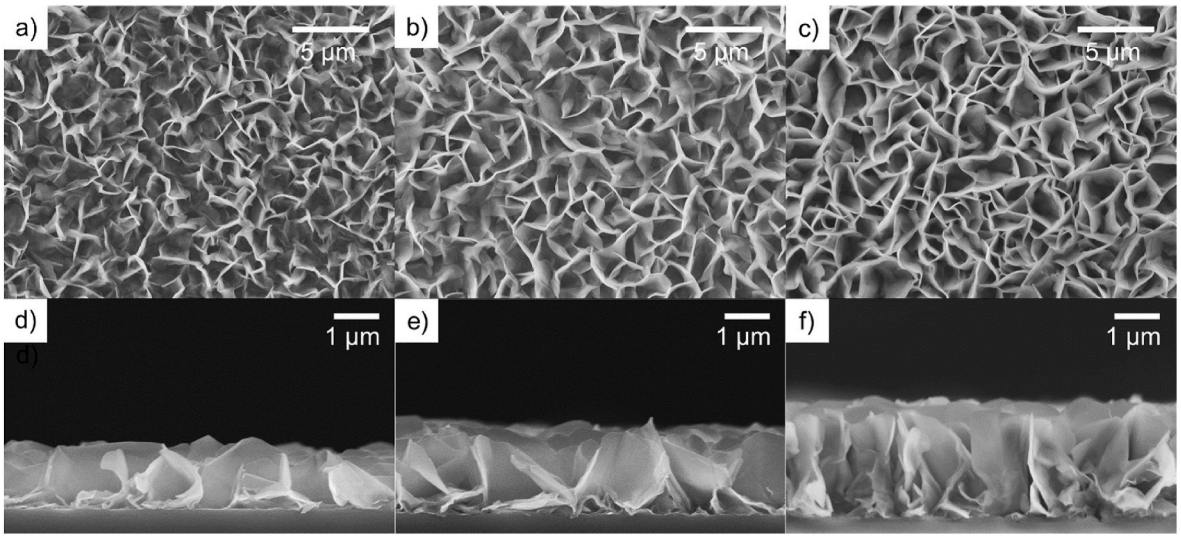

Fig. 1. SEM top view and cross section images of ZnAl(30)-NO_3 (a, d), ZnAl(65)-NO_3 (b, e) and ZnAl(140)-NO_3 (c, f).

c-direction favoured the perpendicular orientation for ZnAl(140)-NO_3 (Fig. 1c,f) in accordance with the proposed "evolution selection" growth mechanism [10]. Looking at higher magnification at the cross-section SEM images (SI-Fig.1), one can distinguish the interlayer between the film and the substrate showing the Al precursor layer had not totally reacted and served as an adhesive layer to the substrate.

Fig. 2 presents the XRD patterns of the ZnAl–NO_3 LDH films. The characteristic reflections of LDH materials were observed and indexed assuming R-3m space group. The (003) and (006) basal reflections were located at 9.98° and 19.96° with a basal spacing of 8.87 Å in accordance with the intercalation of nitrate anions [23]. The calculated d_{003} suggested a "tilt-lying" orientation for the nitrate anions in the interlayer galleries [35,36]. The lattice parameter *a*, corresponding to metal-metal distance was evaluated at 3.07 Å with the (110) reflections. As the film

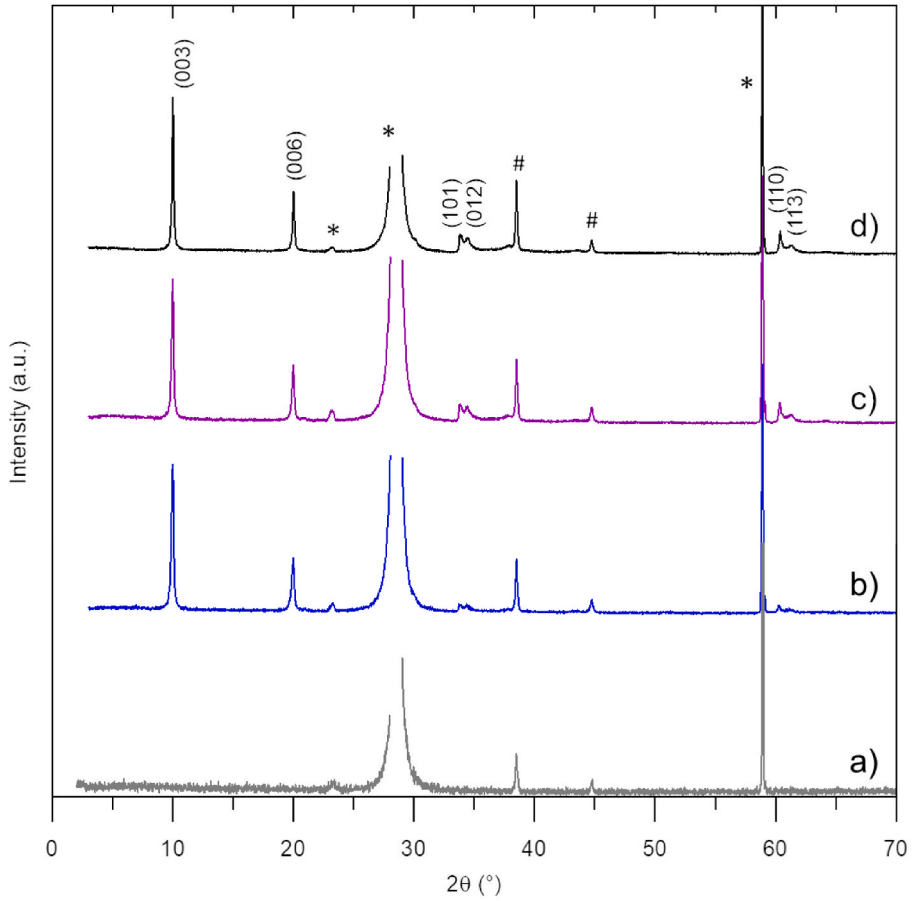

Fig. 2. XRD patterns of (a) the Si substrate, (b) ZnAl(30)-NO_3, (c) ZnAl(65)-NO_3 and (d) ZnAl(140)-NO_3. Peaks associated with the Si substrate (*) and the XRD sample holder (#) are labelled in the patterns.

became thicker, the FWHM of the 00*l* reflections decreased showing the slight increase of particle thickness with the film growth (Table 1). Using the Debye Scherrer equation, the size of the coherent domains relative to the *c*-direction was evaluated for the different films (Table 1). Sizes between 38 and 50 nm were calculated in agreement with the evolution observed on SEM images.

The nature of the interlayer anion was confirmed by Raman spectroscopy. Raman spectra (Fig. 3) show bands at 492 and 550 cm^{-1} assigned to the vibrational modes of the brucitic sheets [37]. Several vibrations modes associated with nitrate anions were also evidenced: at 1056 cm^{-1} and 1382 cm^{-1} assigned to the symmetric (ν_1) and antisymmetric (ν_3) stretching modes, respectively, and at 718 cm^{-1} corresponding to a deformation mode ν_4^{38}. The presence of carbonate anions was excluded as the symmetric stretching of CO_3^{2-} expected at 1062 cm^{-1} was not present (SI-Fig. 2). From XRD and Raman spectroscopy, one can conclude that only nitrate anions occupied the interlayer space of the ZnAl LDH coatings with a "tilt-lying" configuration.

Finally, the chemical composition of the ZnAl(65)-NO_3 coating was determined by EDX and XPS. The Zn:Al ratio was estimated close to 2 as shown in SI-Figs. 3 and 4. ICP-MS was also used to evaluate the amount of LDH on each substrate. Zn and Al were quantified after dissolution of the whole coating in acidic solution (SI-Table 2). The calculated Zn:Al ratios were between 1.1 and 1.4 (lower than the expected value of 2) demonstrating again that a layer of Al was still present between the substrate and the film. This interlayer was demonstrated to play an important role in the adhesion properties of the LDH coating [10] and would need a precise control for practical applications.

3.2. Intercalation properties

3.2.1. Effect of the LDH film thickness

When functionalising LDH coatings, the concentration of anion that could be intercalated is an important parameter to consider as it will dictate the following properties and efficiency of the modified coating. This concentration may be adjusted either by modulating the charge of the LDH sheets or by tuning the coating thickness. The thicker the coating is, the more functional anions will be intercalated. It could also be an advantage for extending the release time of a functional compound considering the diffusion into the film.

For this reason, the intercalation was attempted using the different ZnAl–NO_3 films. Nitrate intercalated LDH were commonly used as precursors for anion exchange considering their low affinity towards the sheets [20]. The intercalation of benzoate anions was first attempted in view of its size (SI-Table 1) but mostly considering its proven antibacterial and antifungal activity regarding different strains [38–41].

After anion exchange with benzoate anions (BZ) and washing, the ZnAl(30)-BZ and ZnAl(65)-BZ films did not change visually. However, when the ZnAl(140)-NO_3 film was considered for anion exchange, the detachment of the LDH film from the substrate was observed after a few minutes. After washing, the film was almost entirely removed (SI-Fig. 5).

Morphological changes resulting from the intercalation of benzoates within ZnAl(140)-NO_3 film were evaluated by SEM (Fig. 4a-b). The images showed the film was pulled out during the anion exchange. The mechanical stress induced by the intercalation of larger molecules than nitrate anions started with the appearance of cracks on the film surface.

Table 1
FWHM of the (003) reflection and sizes of the coherent domains (L_{003}) determined from XRD using Debye-Scherrer equation for the different ZnAl–NO_3 coatings.

	FWHM (003) (degrees)	L_{003} (Å)
ZnAl(30)-NO_3	0.210	379
ZnAl(65)-NO_3	0.194	411
ZnAl(140)-NO_3	0.160	498

In the following, we therefore focus on the behaviour of the ZnAl(30) and ZnAl(65) films.

For ZnAl(30) (SI-Fig. 6) and ZnAl(65) (Fig. 5a, d) films, the microstructure of the film was not modified by the anion exchange. The film surface appeared homogeneous with no sign of mechanical stress. The platelet thickness slightly increased with the benzoate intercalation from 60 nm to 90 nm approximately (from SEM images) suggesting an increase of the interlayer space.

After anion exchange (Fig. 6 and SI-Fig. 7), the (003) and (006) basal reflections shifted down from 9.98° and 19.96° to 5.75° and 11.49° for the ZnAl(30) and ZnAl(65) coatings (Table 2) and higher order (00*l*) reflections appeared resulting from the interlayer space expansion. The intercalation of benzoate led to an increased disorder in the stacking sequence as depicted by the broadening of the reflections in the 30°–40° region. The (003) basal reflection at 9.98° corresponding to ZnAl–NO_3 was still noticed after exchange on both films. Considering its low intensity, only a few nitrate anions, probably those located deep into the film, were not exchanged and remained in the films. The d-values calculated for ZnAl-BZ films (around 15.37 Å, Table 2) were in agreement with previous works reporting the formation of intertwined single layers of benzoate molecules with their anionic groups attached to the OH of the layers via strong hydrogen bonds [42–44]. Whereas ZnAl(30) and ZnAl(65) LDH films were able to withstand an increase of 73 % in d spacing, ZnAl(140) coating did not stand such an expansion due to higher density of particles and their thickness. Note that the (003) reflection was broader than the (006) one suggesting a degree of disorder of the intertwinned layers of benzoate anions in the interlayer space. As a consequence, the evolution of the size of the coherent domains with the intercalation of larger anions was difficult to relate to the change in particle size.

To confirm the anion exchange, infrared transmission spectra of the films on its substrate were recorded before and after intercalation (Fig. 7 and SI-Fig. 8). The vibrational signatures of the LDH matrix was characterized by the O–H stretching band between 3200 and 3600 cm^{-1}, and by a group of bands between 400 and 800 cm^{-1} corresponding to the vibrational modes of the brucitic sheets [37]. A small band at 1647 cm^{-1} can be seen in all spectra and corresponds to the H_2O bending mode of the interlayer water molecules.

Before exchange (Fig. 7a), the presence of nitrate anions was characterized by several bands: one at 822 cm^{-1} corresponding to an out-of-plane deformation mode (ν_2), one at 1054 cm^{-1} corresponding to a symmetric stretching mode (ν_1) and two bands at 1358 cm^{-1} and 1438 cm^{-1} assigned to antisymmetric stretching vibrations (ν_3) of hydrated ions [36,45]. The activation of the ν_1 mode and the splitting of the ν_3 mode proved the "tilt-lying" configuration of the nitrate anions with C_{2v} symmetry [35,36]. Those bands disappeared for the LDH films after anion exchange (Fig. 7b) attesting that less than 5 % of nitrate remained in the material.

After anion exchange with benzoate anions (Fig. 7 b and SI-Fig. 8a), three intense bands can be seen: at 1399 and 1535 cm^{-1} assigned to the symmetric and antisymmetric stretching modes of the carboxylate group [43] and at 1594 cm^{-1} assigned to the a ring stretching vibration of the aromatic ring. These three bands are slightly asymmetric suggesting the presence of carboxylates interacting in different ways with the hydroxide sheets. The shoulder emerging at 3619 cm^{-1} could be assigned to hydroxyl stretching with weak H-bonding interaction.

The exchange between nitrate and benzoate anions was effective into ZnAl(30) and ZnAl(65) LDH films. Note that the anion exchange in the ZnAl(140) LDH was also evidenced by IR spectroscopy (SI-Fig. 8b) confirming the film detachment resulted from the intercalation of bigger anions.

3.2.2. Effect of the anion size

As we evidenced the intercalation of anions into LDH films can be constrained by the film morphology, the intercalation of larger monovalent anions was tested into ZnAl(65)-LDH films. In LDH materials, the

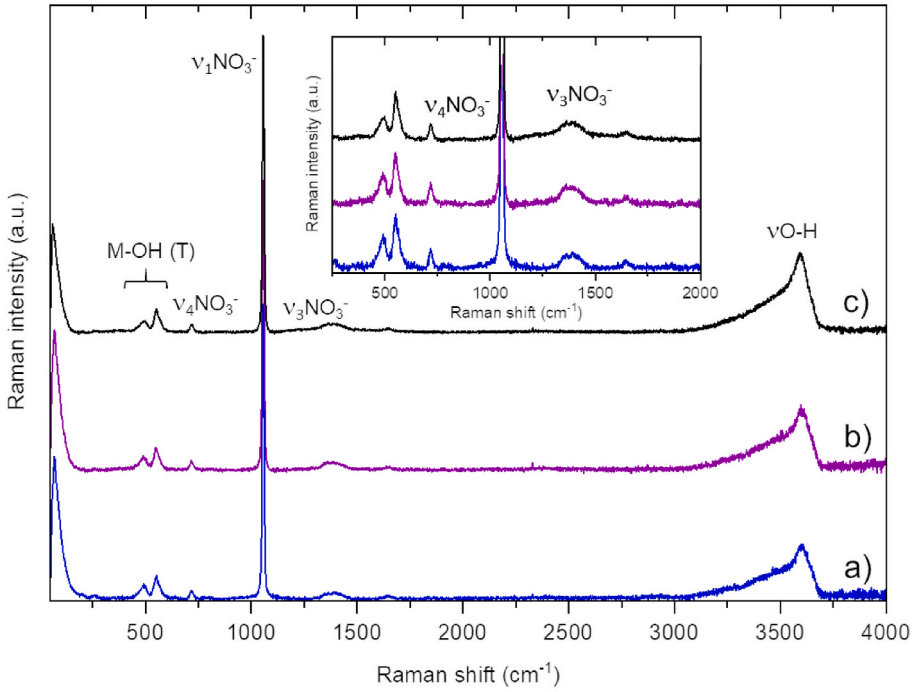

Fig. 3. Raman spectra of (a) ZnAl(30)-NO_3, (b) ZnAl(65)-NO_3 and (c) ZnAl(140)-NO_3.

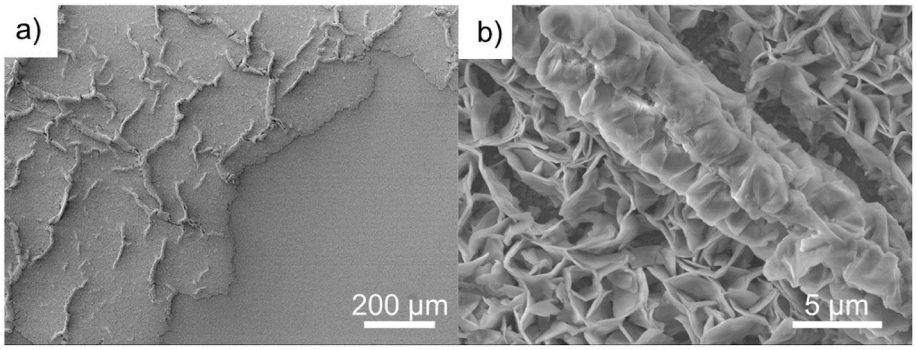

Fig. 4. SEM images of ZnAl(140)-BZ at (a) low and (b) high magnification after intercalation.

Table 2
XRD characteristics measured from the XRD patterns: 2θ values (°) for the (003) and (006) reflections, the corresponding d-value calculated using the Bragg equation, the anion orientation and the interlayer space expansion.

Sample name	$2\theta_{003}$ (°)	$2\theta_{006}$ (°)	d-value (Å)	Corresponding interlayer anion	% expansion
ZnAl(65)-NO_3	9.98	19.96	8.87	"tilt-lying" nitrate	–
ZnAl(65)-BZ	5.75 9.98	11.49 –	15.37 8.86	Intertwined single layer of benzoate "tilt-lying" nitrate	73 –
ZnAl(65)-CFX	5.10 9.45	10.00 –	17.50 9.35	Hydrolysis product of cefotaxime Nitrate	98 –
ZnAl(65)-C8	3.88° 4.46° 9.99°	7.76° 9.26° –	22.75 19.54 8.85	Hydrated monolayer of octanoate Monolayer of octanoate "tilt-lying" nitrate	157 120 –

space between layers is related to both the size and the arrangement mode of the interlayer anions. The anion exchange with cefotaxime (SI-Table 1), which is an antibiotic recommended for the treatment of many kinds of bacterial infections, was attempted. The SEM images of the ZnAl (65)-CFX (Fig. 5b, e) evidenced the microstructure was maintained with the exchange but the LDH platelets appeared clearly thicker suggesting the expansion of the interlayer space.

Looking at the XRD pattern of ZnAl(65)-CFX (Fig. 6b, e), the main basal reflections (003) and (006) shifted down to 5.10° and 10.00° and (009) and (0012) reflections appeared all proving the expansion of the interlayer space (Table 2). The associated FWHM had increased compared to the pristine film implying either higher disorder and/or the decrease of the size of the coherent domains with cefotaxime intercalation. The latter phenomenon had already been observed in LDH powders with the intercalation of vanadates leading to a mechanical fragmentation of the crystallites [46]. The XRD pattern showed an additional peak at 9.45° which may be associated with nitrates. The calculated d-value of 17.50 Å for ZnAl(65)-CFX (Table 2) was significantly lower compared to the one we previously reported for ZnAl LDH particles intercalating cefotaxime (around 20.80 Å) [26]. The molecular form of cefotaxime may have changed with the intercalation in the ZnAl (65)-LDH film or either there could be different hydrated state for this compound or different conformation of the anion in the interlayer space. After exchanging the nitrate anions with cefotaxime, the appearance of multiple bands in the 1000–1800 cm^{-1} region, corresponding to

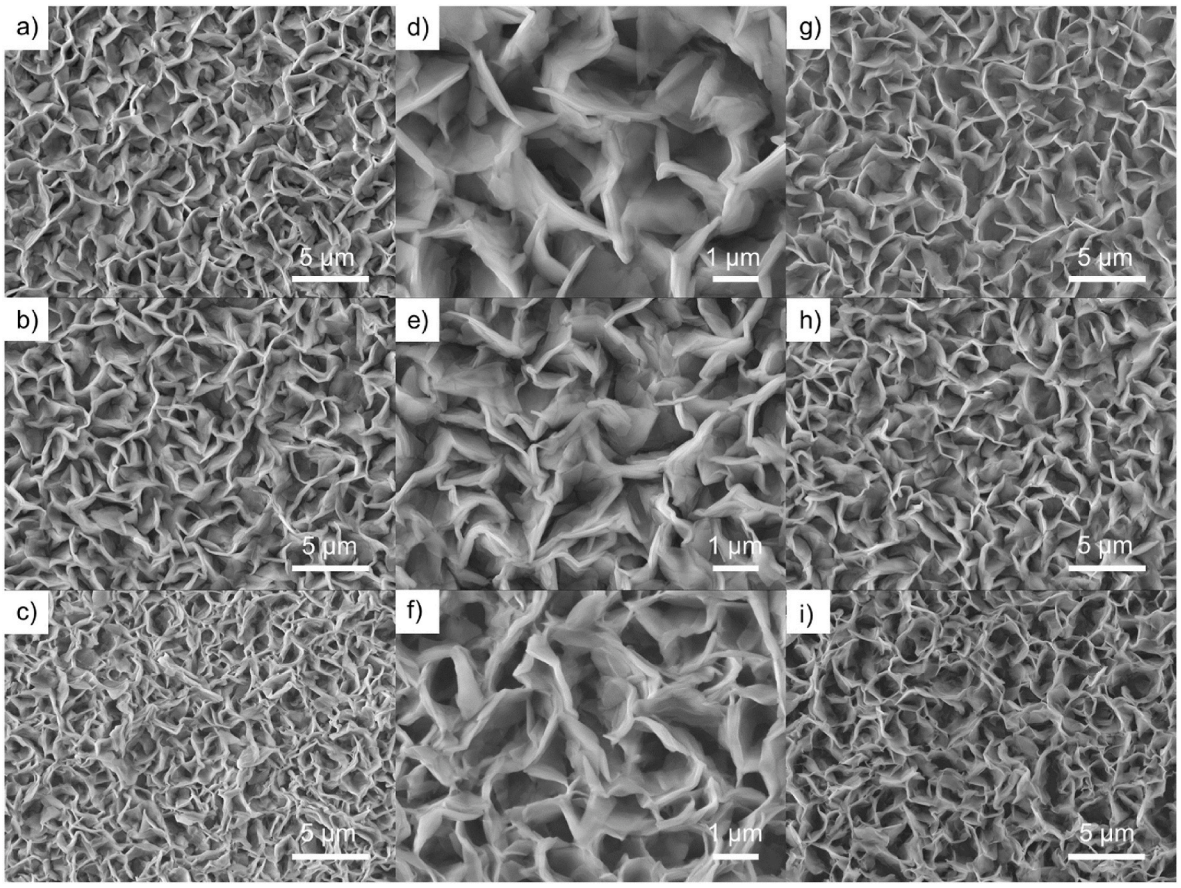

Fig. 5. SEM images at low and high magnification of the functionalised films ZnAl(65)-BZ (a, d), ZnAl(65)-CFX (b, e) and ZnAl(65)-C8 (c, f) and the corresponding image (g, h, i) after immersion for 3 h in physiological saline solution.

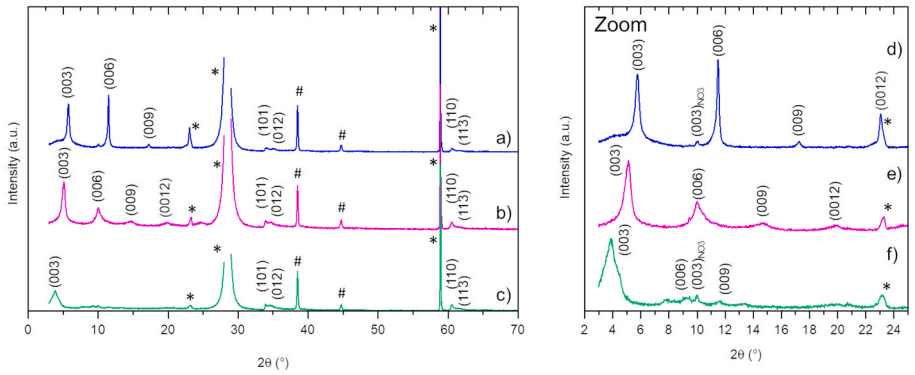

Fig. 6. XRD patterns and a zoom in the 2–25° region of ZnAl(65)-BZ (a, d), ZnAl(65)-CFX (b, e) and ZnAl(65)-C8 (c, f).

vibration modes of cefotaxime (Fig. 7c) were observed. Two main signals changed by comparison with the spectrum of the cefotaxime salt in solution (SI-Fig. 9b). First, the intensity of the band at 1761 cm^{-1} related to the C═O bond of the β-lactam was decreased. Moreover, the signals at around 1250 cm^{-1} assigned to C–O stretching vibrations were significantly lower for the intercalated anion.

XRD and IR spectroscopy both suggested the intercalated anion in ZnAl(65)-LDH was different from the native cefotaxime sodium salt. The hydrolysis of the β-lactam ring leading to its opening was previously studied [47] and Zn(II) complexes were reported to catalyse the reaction [48]. However, as we did not observe this effect when intercalating cefotaxime into ZnAl LDH particles, the constrained dynamics of LDH sheets could explain the change in molecular structure.

To investigate further the limitation in terms of interlayer space expansion in the ZnAl(65) film, the intercalation of octanoate was studied (SI-Table 1). The intercalation of such anion could be interesting for obtaining superhydrophobic properties and limit the adhesion and fouling of the coating. The intercalation of laurate anions had already been reported for ZnAl–NO_3 LDH film grown on Al substrates [23,24] proving the interlamellar space can be expanded to d-values as high as 34 Å depending on the starting film. However, it always resulted in morphological changes of the LDH film.

While the main microstructure was preserved after anion exchange with octanoate as shown by SEM images (Fig. 5c, f), the platelet thickness noticeably increased and at the same time delamination seemed to appear leading to a more disordered the surface. The XRD pattern

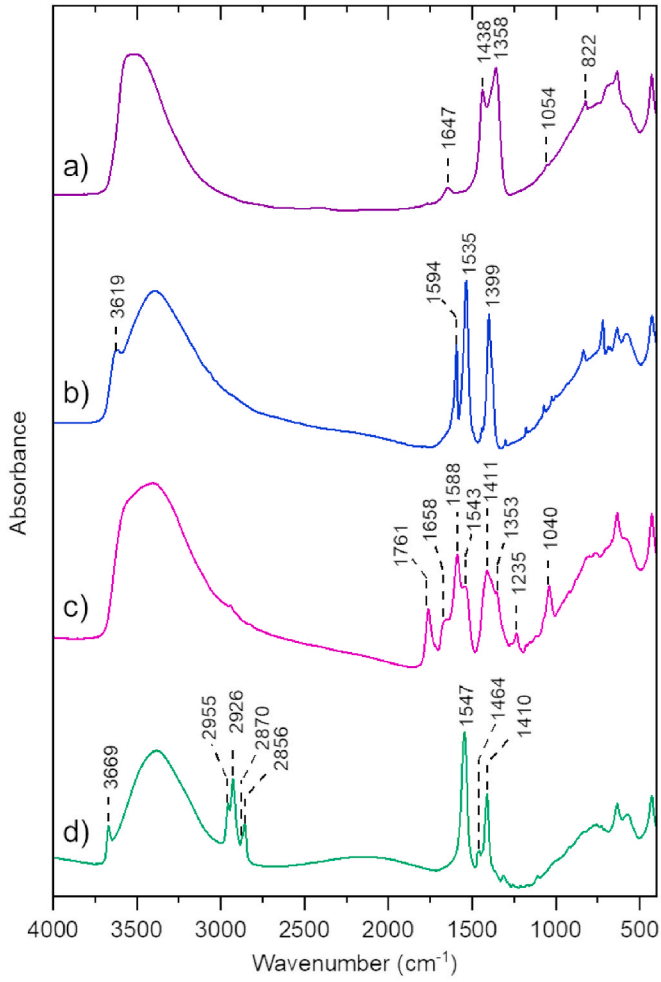

Fig. 7. FTIR transmission spectra of (a) ZnAl(65)-NO_3, (b) ZnAl(65)-BZ, (c) ZnAl(65)-CFX and (d) ZnAl(65)-C8.

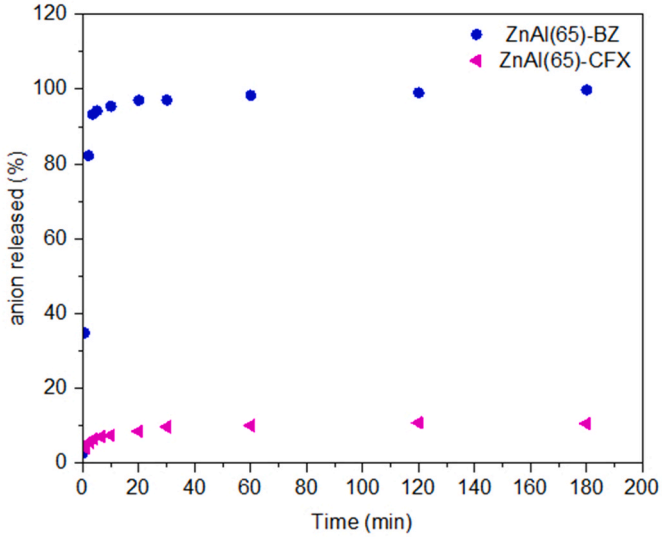

Fig. 8. Anion exchange kinetics evaluated from UV spectrophotometry for ZnAl (65)-BZ (circles) and ZnAl(65)-CFX (triangles).

(Fig. 6c, f) showed one large peak around 4° with several low intensity reflections in the range 6–14°. Two sets of (00*l*) basal reflections were identified with again the presence of the (003) reflections associated

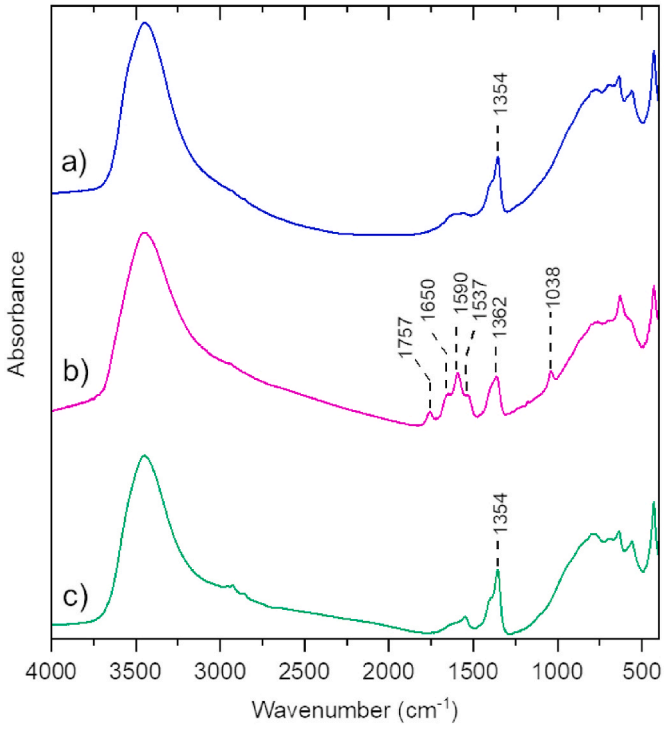

Fig. 9. FTIR transmission spectra of (a) ZnAl(65)-BZ, (b) ZnAl(65)-CFX and (c) ZnAl(65)-C8 after 3 h of immersion in physiological saline solution.

with nitrate anions (Table 2). The calculated d-values were 19.54 Å and 22.75 Å. The former value was in agreement with the literature [49,50], and it was assigned to a monolayer arrangement of the anion. The latter could correspond to another hydration state of the anion. The broadness of the (00*l*) reflections with relatively low intensity may be the result of a disordered arrangement of the octanoate anions in the interlayer space.

The FTIR spectrum (Fig. 7d) displayed an intense couple of bands around ~2930 and 2860 cm^{-1} corresponding to the symmetric and the antisymmetric stretching of CH_2 and CH_3 with the scissoring mode $\delta(CH_2)$ at 1464 cm^{-1}. The absorption bands at 1547 cm^{-1} and 1410 cm^{-1} were assigned to the stretching modes of the carboxylate group. The spectrum revealed no remaining intercalated nitrate. The sharp band at 3669 cm^{-1}, as already seen for ZnAl(65)-BZ (Fig. 7b), was attributed to the stretching of hydroxyl groups with less interaction with the octanoate anions.

3.3. Stability of the functionalised coatings

The stability of the functionalised films was then investigated by immersion in physiological saline solution (0.9 wt % NaCl). The exchange kinetics were followed by the recording of UV spectra of the solution and the acquisition of IR transmission spectra of the film on its substrate after 3 h of immersion.

For ZnAl(65)-BZ, a burst release of benzoate was observed and after 20 min, a plateau was reached evidencing the fast exchange kinetics and release of the benzoate anions in solution (Fig. 8). Based on the estimated Zn amount in ZnAl(65) LDH film by ICP-MS (SI-Table 2), all benzoate anions were exchanged. The release process was not limited by diffusion through the particle forming the film. The coating microstructure was not modified but the thickness of the particles decreased (to around 60 nm from SEM) suggesting the interlayer space was reduced with the exchange (Fig. 5g).

The bands associated with benzoate anions disappeared on the IR spectrum and a new band at 1354 cm^{-1} was evidenced corresponding to the antisymmetric stretching of carbonates (Fig. 9a). Chloride anions may have also been intercalated. The exchange process from the ZnAl

(65)-BZ coating was significantly different compared to the one observed for LDH powders. Indeed, Zhang et al. [40] demonstrated a slow and sustained release process of benzoate anions from ZnAl LDH nanoparticles in NaCl 3.5 wt% without total exchange. However, release properties of LDH can be significantly affected by the aggregation state [51], the particle size [52] and also the packing mode of the anions. In fact, a complex interplay between the anion-host interactions, anion-anion interactions in the interlayer space, and anion affinity towards the medium governed the anions release in LDH materials [53]. Considering (i) the saline solution was not carbonate-free and (ii) the low amount of anion to exchange in the coating, the rapid release of benzoate anions from ZnAl(65)-BZ was not surprising.

When immersing ZnAl(65)-CFX, only few anions (around 10 %) were released from the interlayer space after 3 h. Prolonging the immersion to 18 h did not result in a higher release (data not shown). The coating did not change after immersion (Fig. 5h). Notably the thickness of the platelet was preserved. The IR spectrum (Fig. 9b) evidenced a decrease in intensity of the main bands located in the region 1000-1900 cm^{-1} associated with cefotaxime. However, its spectral signature was still present supporting the partial hydrolysis of the starting cefotaxime leading to an anion with stronger interaction with the hydroxide layers limiting the exchange with the external medium.

For ZnAl(65)-C8, the anion exchange was monitored only from the film features by IR spectroscopy, octanoate having no UV absorbance in the range 200–400 nm. With the immersion time (SI-Fig. 10), one can see the intensity of the main bands corresponding to octanoate anions decreasing while a new band appeared at 1354 cm^{-1} attributed to carbonates. After 3 h of immersion (Fig. 9c), almost all octanoate anions had been replaced. The release rate in this case was lower compared to ZnAl(65)-BZ which may be related to the lower solubility. The film microstructure was slightly altered by the octanoate release (Fig. 5i). The platelet thickness decreased in accordance with the intercalation of the smaller carbonate anions but at the same time, some particles were detached as evidenced by areas on where the substrate was visible. Longer-term stability was achieved by the groups of Cao [24] and Duan [8] with ZnAl-laurate films which could be the result of better anion arrangement in the interlayer space as suggested by XRD.

Even the relatively rapid release occurred for ZnAl(65)-BZ and ZnAl (65)-C8, physical modifications could allow to either slow down the rate (i.e. by depositing a polymer upper layer) or stop the anion exchange process (i.e. by grafting).

3.4. Reloading capacity

The possibility to reload the film for release systems or to regenerate the coating when using for uptake could be very important for practical applications. The coating regeneration was attempted using the method proposed by Iyi et al. [33] using an acid-alcohol mixed solution. While taking advantage of the higher acid resistance of the LDH in alcohols than in water, this method allows a complete decarbonation yielding LDH containing the conjugated base anions of the acids used. The SEM images after immersion into an ethanol-HNO_3 solution displayed an LDH coating with a morphology and microstructure similar to the starting ZnAl(65)-NO_3 (SI-Fig. 11). On the IR spectrum (SI-Fig. 12), the band associated with carbonate anions disappeared and two new bands located at 1358 cm^{-1} and 1441 cm^{-1} corresponding to the stretching vibration of hydrated nitrate anions. The regeneration of the coating was successful and functionalisation could be completed again.

4. Conclusions

ZnAl LDH coatings with controlled morphology and thickness were synthesized by an *in situ* approach. The density of particles as well as the particle size were adjusted by varying the thickness of the Al-precursor layer. The anion exchange properties and dynamics were then studied using SEM, XRD and IR spectroscopy. The influence of the initial film morphology on the anion exchange in such films was highlighted. After optimising the starting film morphology, the intercalation of three functional anions with potential antimicrobials properties was successfully achieved with the possibility to expand the interlayer space up to 150 % while holding the film integrity. The rapid release of the intercalated anions upon immersion in aqueous solution could be improved by physical modifications depending of the target application (polymer upper layer, anion immobilization by grafting). The regeneration capacity of the film was demonstrated as it could be key for practical applications. The objective of this work was to study from a fundamental perspective the intercalation properties of such LDH films but additional work will be necessary to demonstrate the application and determine the functionality of the loaded and released anions.

CRediT authorship contribution statement

S. Soulé: Conceptualization, Investigation, Project administration, Validation, Writing – original draft, Writing – review & editing. **P. Durand:** Investigation, Writing – review & editing. **S. El-Kirat-Chatel:** Investigation, Writing – review & editing. **F. Quilès:** Investigation, Writing – review & editing. **C. Carteret:** Investigation, Writing – review & editing.

Declaration of competing interest

The authors declare that they have no known competing financial interests or personal relationships that could have appeared to influence the work reported in this paper.

Data availability

Data will be made available on request.

Acknowledgements

We would like to acknowledge the SMI spectroscopy and microscopy Service Facility of LCPME (Université de Lorraine-CNRS). Claire Genois from LCPME is particularly acknowledged for the ICP-MS analysis. The authors thank the PMD2X X-ray diffraction facility at Université de Lorraine, for X-ray diffraction measurements.

Appendix A. Supplementary data

Supplementary data to this article can be found online at https://doi.org/10.1016/j.mtchem.2024.101897.

References

[1] M. Xu, M. Wei, Layered double hydroxide-based Catalysts: eecent advances in preparation, structure, and applications, Adv. Funct. Mater. 28 (47) (2018) 1802943, https://doi.org/10.1002/adfm.201802943.
[2] L. Lv, Z. Yang, K. Chen, C. Wang, Y. Xiong, 2D layered double hydroxides for oxygen evolution reaction: from fundamental design to application, Adv. Energy Mater. 9 (17) (2019) 1803358, https://doi.org/10.1002/aenm.201803358.
[3] M. Shao, R. Zhang, Z. Li, M. Wei, D.G. Evans, X. Duan, Layered double hydroxides toward electrochemical energy storage and conversion: design, synthesis and applications, Chem. Commun. 51 (88) (2015) 15880–15893, https://doi.org/10.1039/C5CC07296D.
[4] N. Chubar, R. Gilmour, V. Gerda, M. Mičušík, M. Omastova, K. Heister, P. Man, J. Fraissard, V. Zaitsev, Layered double hydroxides as the next generation inorganic anion exchangers: synthetic methods versus applicability, Adv. Colloid Interface Sci. 245 (2017) 62–80, https://doi.org/10.1016/j.cis.2017.04.013.
[5] T. Hu, Z. Gu, G.R. Williams, M. Strimaite, J. Zha, Z. Zhou, X. Zhang, C. Tan, R. Liang, Layered double hydroxide-based nanomaterials for biomedical applications, Chem. Soc. Rev. 51 (14) (2022) 6126–6176, https://doi.org/10.1039/D2CS00236A.
[6] J.L. Paulhiac, O. Clause, Surface coprecipitation of cobalt(II), nickel(II), or zinc(II) with aluminum(III) ions during impregnation of .Gamma.-Alumina at neutral PH, J. Am. Chem. Soc. 115 (24) (1993) 11602–11603, https://doi.org/10.1021/ja00077a071.

[7] J.-B. d'Espinose de la Caillerie, M. Kermarec, O. Clause, Impregnation of .Gamma.-Alumina with Ni(II) or Co(II) ions at neutral PH: hydrotalcite-type coprecipitate formation and characterization, J. Am. Chem. Soc. 117 (46) (1995) 11471–11481, https://doi.org/10.1021/ja00151a010.

[8] H. Chen, F. Zhang, S. Fu, X. Duan, In situ microstructure control of oriented layered double hydroxide monolayer films with curved hexagonal crystals as superhydrophobic materials, Adv. Mater. 18 (23) (2006) 3089–3093, https://doi.org/10.1002/adma.200600615.

[9] L. Wang, Q. Zong, W. Sun, Z. Yang, G. Liu, Chemical modification of hydrotalcite coating for enhanced corrosion resistance, Corrosion Sci. 93 (2015) 256–266, https://doi.org/10.1016/j.corsci.2015.01.033.

[10] X. Guo, S. Xu, L. Zhao, W. Lu, F. Zhang, D.G. Evans, X. Duan, One-step hydrothermal crystallization of a layered double hydroxide/alumina bilayer film on aluminum and its corrosion resistance properties, Langmuir 25 (17) (2009) 9894–9897, https://doi.org/10.1021/la901012w.

[11] J. Liu, Y. Li, X. Huang, G. Li, Z. Li, Layered double hydroxide nano- and microstructures grown directly on metal substrates and their calcined products for application as Li-ion battery electrodes, Adv. Funct. Mater. 18 (9) (2008) 1448–1458, https://doi.org/10.1002/adfm.200701383.

[12] L. Wu, D. Yang, G. Zhang, Z. Zhang, S. Zhang, A. Tang, F. Pan, Fabrication and characterization of Mg-M layered double hydroxide films on anodized magnesium alloy AZ31, Appl. Surf. Sci. 431 (2018) 177–186, https://doi.org/10.1016/j.apsusc.2017.06.244.

[13] X. Lei, B. Wang, J. Liu, Z. Ye, Z. Chang, M. Jiang, X. Sun, Three-dimensional NiAl-mixed metal oxide film: preparation and capacitive deionization performances, RSC Adv. 4 (78) (2014) 41642–41648, https://doi.org/10.1039/C4RA08415B.

[14] Y. Liu, N. Wang, J.H. Pan, F. Steinbach, J. Caro, In situ synthesis of MOF membranes on ZnAl-CO3 LDH buffer layer-modified substrates, J. Am. Chem. Soc. 136 (41) (2014) 14353–14356, https://doi.org/10.1021/ja507408s.

[15] X. Guo, F. Zhang, S. Xu, D.G. Evans, X. Duan, Preparation of layered double hydroxide films with different orientations on the opposite sides of a glass substrate by in situ hydrothermal crystallization, Chem. Commun. 44 (2009) 6836, https://doi.org/10.1039/b911216b.

[16] Z. Lü, F. Zhang, X. Lei, L. Yang, D.G. Evans, X. Duan, Microstructure-controlled synthesis of oriented layered double hydroxide thin films: effect of varying the preparation conditions and a kinetic and mechanistic study of film formation, Chem. Eng. Sci. 62 (21) (2007) 6069–6075, https://doi.org/10.1016/j.ces.2007.06.037.

[17] M.S. Yarger, E.M.P. Steinmiller, K.-S. Choi, Electrochemical synthesis of Zn−Al layered double hydroxide (LDH) films, Inorg. Chem. 47 (13) (2008) 5859–5865, https://doi.org/10.1021/ic800193j.

[18] Z. Li, M. Shao, H. An, Z. Wang, S. Xu, M. Wei, D.G. Evans, X. Duan, Fast electrosynthesis of Fe-containing layered double hydroxide arrays toward highly efficient electrocatalytic oxidation reactions, Chem. Sci. 6 (11) (2015) 6624–6631, https://doi.org/10.1039/C5SC02417J.

[19] F. Zhang, M. Sun, S. Xu, L. Zhao, B. Zhang, Fabrication of oriented layered double hydroxide films by spin coating and their use in corrosion protection, Chem. Eng. J. 141 (1) (2008) 362–367, https://doi.org/10.1016/j.cej.2008.03.016.

[20] S. Miyata, Anion-exchange properties of hydrotalcite-like compounds, Clay Clay Miner. 31 (4) (1983) 305–311, https://doi.org/10.1346/CCMN.1983.0310409.

[21] S.K. Poznyak, J. Tedim, L.M. Rodrigues, A.N. Salak, M.L. Zheludkevich, L.F.P. Dick, M.G.S. Ferreira, Novel inorganic host layered double hydroxides intercalated with guest organic inhibitors for anticorrosion applications, ACS Appl. Mater. Interfaces 1 (10) (2009) 2353–2362, https://doi.org/10.1021/am900495r.

[22] J. Tedim, M.L. Zheludkevich, A.C. Bastos, A.N. Salak, A.D. Lisenkov, M.G. S. Ferreira, Influence of preparation conditions of layered double hydroxide conversion films on corrosion protection, Electrochim. Acta 117 (2014) 164–171, https://doi.org/10.1016/j.electacta.2013.11.111.

[23] F. Zhang, L. Zhao, H. Chen, S. Xu, D.G. Evans, X. Duan, Corrosion resistance of superhydrophobic layered double hydroxide films on aluminum, Angew. Chem. 120 (13) (2008) 2500–2503, https://doi.org/10.1002/ange.200704694.

[24] Y. Cao, D. Zheng, X. Li, J. Lin, C. Wang, S. Dong, C. Lin, Enhanced corrosion resistance of superhydrophobic layered double hydroxide films with long-term stability on Al substrate, ACS Appl. Mater. Interfaces 10 (17) (2018) 15150–15162, https://doi.org/10.1021/acsami.8b02280.

[25] Y. Cao, D. Zheng, J. Luo, F. Zhang, C. Wang, S. Dong, Y. Ma, Z. Liang, C. Lin, Enhanced corrosion protection by Al surface immobilization of in-situ grown layered double hydroxide films Co-intercalated with inhibitors and low surface energy species, Corrosion Sci. 164 (2020) 108340, https://doi.org/10.1016/j.corsci.2019.108340.

[26] G. Francius, E. André, S. Soulé, C. Merlin, C. Carteret, Layered double hydroxides (LDH) as nanocarriers for antimicrobial chemotherapy: from formulation to targeted applications, Mater. Chem. Phys. 293 (2023) 126965, https://doi.org/10.1016/j.matchemphys.2022.126965.

[27] M.P. Figueiredo, V.R.R. Cunha, F. Leroux, C. Taviot-Gueho, M.N. Nakamae, Y. R. Kang, R.B. Souza, A.M.C.R.P.F. Martins, I.H.J. Koh, V.R.L. Constantino, Iron-based layered double hydroxide implants: potential drug delivery carriers with tissue biointegration promotion and blood microcirculation preservation, ACS Omega 3 (12) (2018) 18263–18274, https://doi.org/10.1021/acsomega.8b02532.

[28] D. Eulálio, M. Pires Figueiredo, C. Taviot-Gueho, F. Leroux, C.H. Dos Reis Serra, D. L. A. de Faria, V.R.L. Constantino, Development of dipeptide N-Acetyl-L-Cysteine loaded nanostructured carriers based on inorganic layered hydroxides, Pharmaceutics 15 (3) (2023) 955, https://doi.org/10.3390/pharmaceutics15030955.

[29] S. Saha, S. Ray, R. Acharya, T.K. Chatterjee, J. Chakraborty, Magnesium, zinc and calcium aluminium layered double hydroxide-drug nanohybrids: a comprehensive study, Appl. Clay Sci. 135 (2017) 493–509, https://doi.org/10.1016/j.clay.2016.09.030.

[30] S. Coiai, F. Cicogna, S. Pinna, R. Spiniello, M. Onor, W. Oberhauser, M.-B. Coltelli, E. Passaglia, Antibacterial LDPE-based nanocomposites with salicylic and rosmarinic acid-modified layered double hydroxides, Appl. Clay Sci. 214 (2021) 106276, https://doi.org/10.1016/j.clay.2021.106276.

[31] D. Wang, F. Peng, J. Li, Y. Qiao, Q. Li, X. Liu, Butyrate-inserted Ni–Ti layered double hydroxide film for H2O2-mediated tumor and bacteria killing, Mater. Today 20 (5) (2017) 238–257, https://doi.org/10.1016/j.mattod.2017.05.001.

[32] C.S. Neves, A.C. Bastos, A.N. Salak, M. Starykevich, D. Rocha, M.L. Zheludkevich, A. Cunha, A. Almeida, J. Tedim, M.G.S. Ferreira, Layered double hydroxide clusters as precursors of novel multifunctional layers: a bottom-up approach, Coatings 9 (5) (2019) 328, https://doi.org/10.3390/coatings9050328.

[33] N. Iyi, H. Yamada, T. Sasaki, Deintercalation of carbonate ions from carbonate-type layered double hydroxides (LDHs) using acid–alcohol mixed solutions, Appl. Clay Sci. 54 (2) (2011) 132–137, https://doi.org/10.1016/j.clay.2011.07.017.

[34] Y. Cao, D. Zheng, C. Lin, Effect of physical barrier and anion-exchange process of nitrate-intercalated ZnAl layered double hydroxide films grown on Al on corrosion protection, Surf. Coat. Technol. 421 (2021) 127436, https://doi.org/10.1016/j.surfcoat.2021.127436.

[35] Z.P. Xu, H.C. Zeng, Abrupt structural transformation in hydrotalcite-like compounds $Mg_{1-x}Al_x(OH)_2(NO_3)_x \cdot n H_2O$ as a continuous function of nitrate anions, J. Phys. Chem. B 105 (9) (2001) 1743–1749, https://doi.org/10.1021/jp0029257.

[36] S.-L. Wang, P.-C. Wang, In situ XRD and ATR-FTIR study on the molecular orientation of interlayer nitrate in Mg/Al-layered double hydroxides in water, Colloids Surf. A Physicochem. Eng. Asp. 292 (2) (2007) 131–138, https://doi.org/10.1016/j.colsurfa.2006.06.014.

[37] J.T. Kloprogge, L. Hickey, R.L. Frost, FT-Raman and FT-IR spectroscopic study of synthetic Mg/Zn/Al-hydrotalcites, J. Raman Spectrosc. 35 (11) (2004) 967–974, https://doi.org/10.1002/jrs.1244.

[38] X. Kang, H. Ye, Antimicrobial alkali-activated slag through self-intercalation of benzoate in layered double hydroxides, Cem. Concr. Compos. 130 (2022) 104533, https://doi.org/10.1016/j.cemconcomp.2022.104533.

[39] G. Mishra, B. Dash, S. Pandey, D. Sethi, C.G. Kumar, Comparative evaluation of synthetic routes and antibacterial/antifungal properties of Zn–Al layered double hydroxides containing benzoate anion, Environ. Eng. Sci. 35 (3) (2018) 247–260, https://doi.org/10.1089/ees.2017.0062.

[40] Y. Wang, D. Synthesis Zhang, Characterization, and controlled release anticorrosion behavior of benzoate intercalated Zn–Al layered double hydroxides, Mater. Res. Bull. 46 (11) (2011) 1963–1968, https://doi.org/10.1016/j.materresbull.2011.07.021.

[41] U. Costantino, V. Bugatti, G. Gorrasi, F. Montanari, M. Nocchetti, L. Tammaro, V. Vittoria, New polymeric composites based on poly(ϵ-caprolactone) and layered double hydroxides containing antimicrobial species, ACS Appl. Mater. Interfaces 1 (3) (2009) 668–677, https://doi.org/10.1021/am8001988.

[42] V. Prévot, C. Forano, J.P. Besse, Hybrid derivatives of layered double hydroxides, Appl. Clay Sci. 18 (1) (2001) 3–15, https://doi.org/10.1016/S0169-1317(00)00025-9.

[43] P. Kovář, M. Pospíšil, M. Nocchetti, P. Čapková, K. Melánová, Molecular modeling of layered double hydroxide intercalated with benzoate, modeling and experiment, J. Mol. Model. 13 (8) (2007) 937–942, https://doi.org/10.1007/s00894-007-0217-4.

[44] M. Meyn, K. Beneke, G. Lagaly, Anion-exchange reactions of layered double hydroxides, Inorg. Chem. 29 (26) (1990) 5201–5207, https://doi.org/10.1021/ic00351a013.

[45] D.J. Goebbert, E. Garand, T. Wende, R. Bergmann, G. Meijer, K.R. Asmis, D. M. Neumark, Infrared spectroscopy of the microhydrated nitrate ions NO3−(H2O)1−6, J. Phys. Chem. A 113 (26) (2009) 7584–7592, https://doi.org/10.1021/jp9017103.

[46] A.N. Salak, J. Tedim, A.I. Kuznetsova, M.L. Zheludkevich, M.G.S. Ferreira, Anion exchange in Zn–Al layered double hydroxides: in situ X-ray diffraction study, Chem. Phys. Lett. 495 (1) (2010) 73–76, https://doi.org/10.1016/j.cplett.2010.06.041.

[47] J. Pitarch, M.F. Ruiz-López, E. Silla, J.-L. Pascual-Ahuir, I. Tuñón, Neutral and alkaline hydrolyses of model β-lactam antibiotics. An ab initio study of water catalysis, J. Am. Chem. Soc. 120 (9) (1998) 2146–2155, https://doi.org/10.1021/ja972801g.

[48] N.V. Kaminskaia, B. Spingler, S.J. Lippard, Hydrolysis of β-lactam antibiotics catalyzed by dinuclear zinc(II) complexes: functional mimics of metallo-β-lactamases, J. Am. Chem. Soc. 122 (27) (2000) 6411–6422, https://doi.org/10.1021/ja993704l.

[49] Z.P. Xu, P. Braterman, S. Synthesis, Structure and morphology of organic layered double hydroxide (LDH) hybrids: comparison between aliphatic anions and their oxygenated analogs, Appl. Clay Sci. 48 (1) (2010) 235–242, https://doi.org/10.1016/j.clay.2009.11.009.

[50] T. Kuehn, H. Poellmann, Synthesis and characterization of Zn-Al layered double hydroxides intercalated with 1- to 19-carbon carboxylic acid anions, Clay Clay Miner. 58 (5) (2010) 596–605, https://doi.org/10.1346/CCMN.2010.0580502.

[51] P. Gunawan, R. Xu, Direct control of drug release behavior from layered double hydroxides through particle interactions, J. Pharm. Sci. 97 (10) (2008) 4367–4378, https://doi.org/10.1002/jps.21321.
[52] X.-Q. Zhang, M.-G. Zeng, S.-P. Li, X.-D. Li, Methotrexate intercalated layered double hydroxides with different particle sizes: structural study and controlled release properties, Colloids Surf. B Biointerfaces 117 (2014) 98–106, https://doi.org/10.1016/j.colsurfb.2014.02.018.
[53] A.I. Khan, A. Ragavan, B. Fong, C. Markland, M. O'Brien, T.G. Dunbar, G. R. Williams, D. O'Hare, Recent developments in the use of layered double hydroxides as host materials for the storage and triggered release of functional anions, Ind. Eng. Chem. Res. 48 (23) (2009) 10196–10205, https://doi.org/10.1021/ie9012612.